Hydrothermal Synthesis of Vanadium Oxides

Thomas Chirayil, Peter Y. Zavalij, and M. Stanley Whittingham*

Chemistry Department and Materials Research Center, State University of New York at Binghamton, Binghamton, New York 13902

Received April 2, 1998. Revised Manuscript Received May 11, 1998

The use of mild hydrothermal methods to synthesize vanadium oxides is reviewed, with particular emphasis on those with layer and 3-dimensional structures. A wide range of studies has been performed predominantly in the past decade to grow new materials that might have interesting electrochemical and magnetic properties. Most emphasis has been placed on vanadium oxides that contain organic species or simple cations such as the alkali metals, alkaline earths, zinc and copper. The key parameters determining the structures formed are reviewed, including pH and the organic structure-directing ion. Some initial electrochemical studies are described.

Contents

Introduction

Hydrothermal synthesis has been extensively used over many decades for the synthesis of zeolites and has been documented by Barrer.[1] In the last 10 years there has been increased activity due to the discovery of the MCM-41 wide-pore compounds at Mobil,[2] and the subsequent effort to synthesize transition metal analogues.[3−8] In 1989, Gunter et al.[9] reported that tungsten trioxide could be formed hydrothermally, and subsequently Reis et al. showed[10] that either the hexagonal or the pyrochlore form of tungsten trioxide could be formed by varying the pH of the reaction medium. A range of tungsten oxides was reported,[11−14] including cluster compounds formed when the tetramethylammonium (TMA) ion was present.[15] In addition, the hydrothermal formation of thin films on conducting substrates was found to be feasible.[16] A number of molybdenum oxides have also been formed by hydrothermal reactions, and this soft chemistry approach allowed for the formation[17] of hexagonal tunnel structure MoO_3 with vacant tunnels.

Although organic cations have been extensively used as templating or structure-directing ions in hydrothermal reactions, little work has been reported on their use in the synthesis of new transition metal oxides. However, an organic molybdenum oxide, $N(CH_3)_4HMo_4O_{12}$, with a new layer structure was reported in 1994,[18] and in the last 3 years there has been much interest in related compounds of the vanadium oxides. Oka and his group have made extensive studies, in the past decade, of the hydrothermal formation of vanadium oxides containing small metal cations. This review discusses this hydrothermal approach to the synthesis of vanadium oxides, and covers both organic- and inorganic-containing vanadium oxides. Emphasis is placed on 2- and 3-dimensional solids and on small cations; 1-dimensional solids are excluded, as are surfactant vanadium oxides and those containing a second nonmetallic element such as vanadium phosphates. The discussion of the mechanism of the growth of these solids from solution has been reviewed by Livage et al.[19−22] and will not be repeated here.

Part of the driving force for the study of new compounds is a constant search for new oxides, which could be used as cathodic materials for advanced lithium batteries. Much of that effort has been focused on new metastable vanadium oxides, as well as on manganese oxides.[23] The structure of the oxide lattice and the possible addition of a second metal might be critical in obtaining reversible lithium intercalation. Indeed, a previous study on a $Fe_{0.11}V_2O_{5.16}$ compound obtained by sol−gel process has shown that the presence of ferric ions in the orthorhombic host lattice induced a real improvement of its electrochemical properties compared with V_2O_5.[24,25] The use of "chimie douce" methods, like hydrothermal,[26] allows new materials, often with open structures, to be obtained that are often not able to be synthesized by using solid-state reactions at high temperature.

Experimental Section

All the materials described here were synthesized by mild hydrothermal synthesis from aqueous solution at temperatures 100−250 °C, and most commonly from

* Corresponding author. Phone and fax: (607) 777-4623. E-mail: stanwhit@binghamton.edu.

10.1021/cm980242m CCC: $15.00
Published on Web 09/24/1998

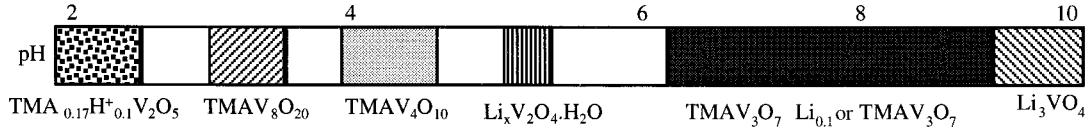

Figure 1. pH dependence of the phases formed when V_2O_5, TMAOH, and LiOH in the molar ratio 1:2:1 are reacted at 185 °C. pH controlled by addition of acetic acid.

Table 1. Crystallographic Data for Hydrothermal Compounds

compound	space group	a (Å)	b (Å)	c (Å)	α (°)	β (°)	γ (°)	ref
$[N(CH_3)_4]V_3O_7$	$P2_1/n$	18.48	6.55	8.43	90	91.1	90	27,38
$Li_{0.6}V_{2-\delta}O_{4-\delta}\cdot H_2O$	$I4/mmm$	3.71	3.71	15.80	90	90	90	33,41
$Li_{0.6}V_{2-\delta}O_{4-\delta}$	$P4/nmm$	3.69	3.69	6.80	90	90	90	42
$[N(CH_3)_4]V_4O_{10}$	$Cmc2_1$	17.12	6.64	11.74	90	90	90	33,54
$[N(CH_3)_4]V_8O_{20}$	$C2/m$	23.66	3.59	6.32	90	103.06	90	28
$[N(CH_3)_4]_5V_{18}O_{46}$	$P\bar{1}$	12.66	15.39	16.96	78.68	74.44	83.46	56
$[N(CH_3)_4]_{0.17}H_{0.1}V_2O_5 \approx$ gel				12.97				29
$(CH_3NH_3)V_3O_7$	$P2_1/c$	11.83	6.66	15.19	90	138.11	90	31
$(CH_3NH_3)_{0.75}V_4O_{10}$	$C2/m$	11.67	3.67	11.10	90	99.87	90	31
$[N(CH_3)_4]_{0.17}[Fe]_{0.17}V_2O_5\cdot 0.17H_2O$	monocli	11.63	3.66	13.70	90	107.18	90	64
$Zn_{0.4}V_2O_5\cdot 0.3H_2O$	$C2/m$	11.74	3.61	10.50	90	96.69	90	63,64
$Zn_3(OH)_2V_2O_7\cdot 2H_2O$	$P3m1$	6.051	6.051	7.195	90	90	120	66
$(C_6H_{14}N_2)V_6O_{14}\cdot H_2O]$	$C2$	19.30	6.66	7.57	90	11.29	90	36,37
$(H_2NCH_2CH_2NH_2)_2Zn[V_6O_{14}]$	$P2_1/n$	9.01	6.53	15.70	90	99.70	90	39
$(H_2NCH_2CH_2NH_2)_2Cu[V_6O_{14}]$	$P2_1/n$	8.93	6.56	15.70	90	99.73	90	39
$[(H_2NCH_2CH_2NH_2)_2Ni]_2[V_3O_7]$	$P2_1/c$	8.93	17.13	6.63	90	111.61	90	40
$[(bpy)_2Zn]_2V_4O_{10}$	$P2_1/a$	10.57	14.73	15.50	90	92.47	90	39
$H_3N(CH_2)_3NH_3V_4O_{10}$	$P2_1/n$	7.999	10.01	15.70	90	100.49	90	60,61
α-$(H_3N(C_2H_4)_2NH_3)_2V_4O_{10}$	$P\bar{1}$	6.39	6.42	8.2	94.51	105.93	104.0	57
β-$(H_3N(C_2H_4)_2NH_3)_2V_4O_{10}$	$P2_1/n$	9.36	6.43	10.39	90	105.83	90	58
α-$(H_3NCH_2CH_2NH_3)V_4O_{10}$	$P\bar{1}$	6.60	7.64	5.98	109.55	104.75	82.31	57
β-$(H_3NCH_2CH_2NH_3)V_4O_{10}$	$P\bar{1}$	6.25	6.40	7.47	78.67	80.16	77.20	58
$[(H_2NCH_2CH_2NH_2)_2Cu]_2V_{10}O_{25}$	$P\bar{1}$	8.93	15.93	6.73	91.12	106.32	105.0	39
VO_2(B)	$C2/m$	12.03	3.69	6.42	90	106.6	90	47
VO_2(A)	$P4_2/ncm$	8.48	8.48	7.62	90	90	90	48
σ-$Zn_{0.25}V_2O_5\cdot H_2O$	$P\bar{1}$	10.61	8.03	10.77	90.65	91.14	90.09	62
$Cs_2V_4O_{11}$	$Cmm2$	5.57	9.64	5.22	90	90	90	98
$V_3O_7\cdot H_2O$	$Pnam$	16.93	9.36	3.64	90	90	90	68
BaV_3O_8	$P2_1$	7.44	5.55	8.20	90	107.2	90	76
$BaV_7O_{16}\cdot H_2O$	$P4_2/m$	6.160	6.160	21.52	90	90	90	80
$M_{0.4}V_3O_8(VO)_{0.4}\cdot nH_2O$	$P2_1/m$	10.15	3.63	9.43	90	102.1	90	78

150 °C to 200 °C. Several parameters are important in the synthesis, in particular the pH of the reaction medium, the ratio of the reactants, the ions present in solution, including shape-directing/templating ions, and the temperature of the reaction. Figure 1 shows the impact of pH for one example,[27,28] that for the reaction of V_2O_5, TMAOH, and LiOH in the molar ratio 1:2:1 at 185 °C for 72 h; the pH was controlled by the addition of acetic acid, which forms an effective buffer with the TMA ions. The organic acid can also act as a reducing agent, and so must be chosen to optimize buffer control vs reduction; thus, for example, propionic acid, CH_3CH_2-COOH, is a more effective reducing agent than acetic acid in leading to the formation of VO_2(B) under the most acidic conditions.[29] Temperature is also critical, so that at 200 °C acetic acid also reduces V_2O_5 to VO_2.[30] The structures of the compounds are discussed in the following pages. When methylamine was substituted for the TMA ion, a different series of compounds was formed.[31,32] The crystallographic data for most of the compounds described in this review are given in Table 1; the specific reaction conditions can be found in the cited references.

Results and Discussion

We will discuss the organic compounds first, and start that discussion with the TMA compounds, as they are the most numerous and were the first hydrothermally prepared compounds[33] with an extended vanadium oxide lattice containing organic species. Figure 1 shows the different compounds formed as a function of the pH of the reaction medium, and Figure 2 shows how the morphology of the compounds formed changes dramatically from plates to fibers, and to large crystallites for cluster compounds {e.g., $TMA_4[V_{22}O_{54}(CH_3COO)]\cdot 4H_2O$},[34] which will not be discussed here but which can be prevalent under normal reaction conditions. At the highest pH values the well-known Li_3VO_4 phase is formed; the vanadium is in tetrahedral coordination. As the pH is reduced the compound $Li_{0.1}TMAV_3O_7$ is found; lithium is not required in the reaction medium, but gives more crystalline material. On heating gently in oxygen, the material takes up one oxygen, giving $TMAV_3O_8$, as shown in Figure 3,[35] before losing the organic and converting to V_2O_5. The V_3O_7 structure is the most prevalent of those found. First described by Nazar et al.[36] for the compound $DABCOV_6O_{14}\cdot H_2O$, which is formed by the hydrothermal reaction of DABCO (1,4-Diazabicyclo[2.2.2]octane) with either $NaVO_3$[36] or V_2O_5,[37] the structure contains both VO_5 square pyramids (SPs) and VO_4 tetrahedra. The SPs share edges to form zigzag chains in the [010] direction, so that two adjacent SPs have the apices up and the next two down. These zigzag chains are connected by corner-

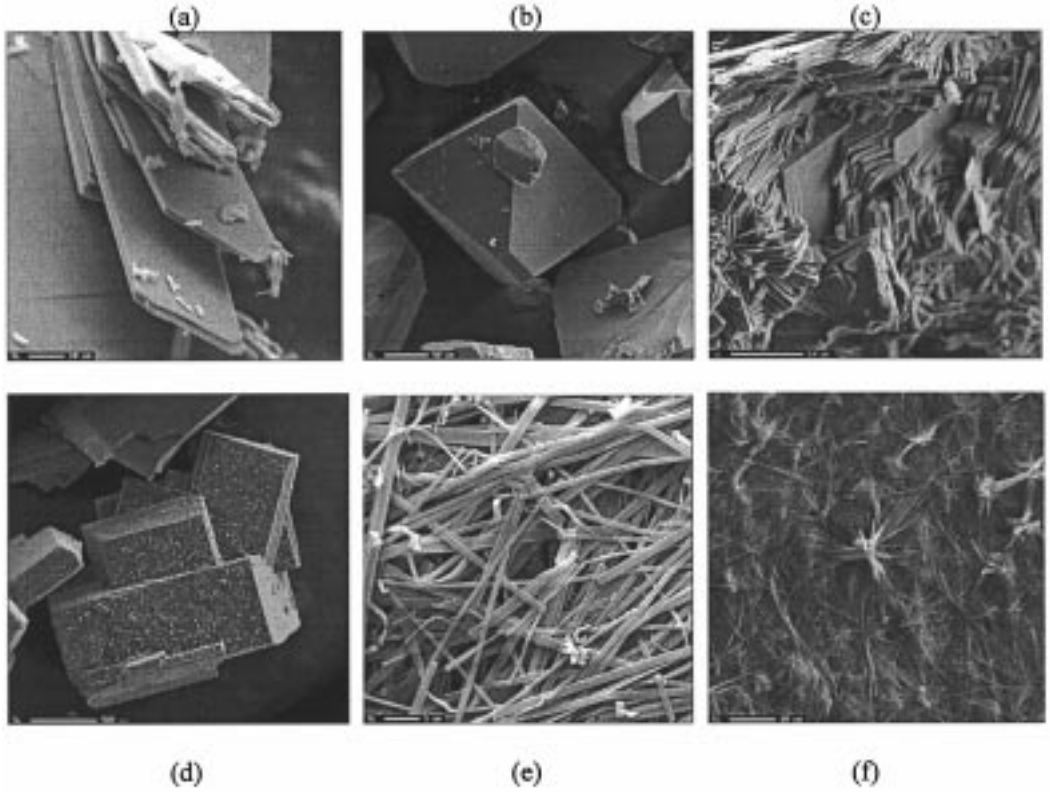

Figure 2. Morphology of the compounds formed at different pH levels: (a) $TMAV_3O_7$, (b) $TMA_4[V_{22}O_{54}(CH_3COO)]\cdot 4H_2O$, (c) $Li_xV_2O_4\cdot H_2O$, (d) $TMAV_4O_{10}$, (e) $TMAV_8O_{10}$, and (f) $TMA_{0.17}H_{0.1}V_2O_5$.

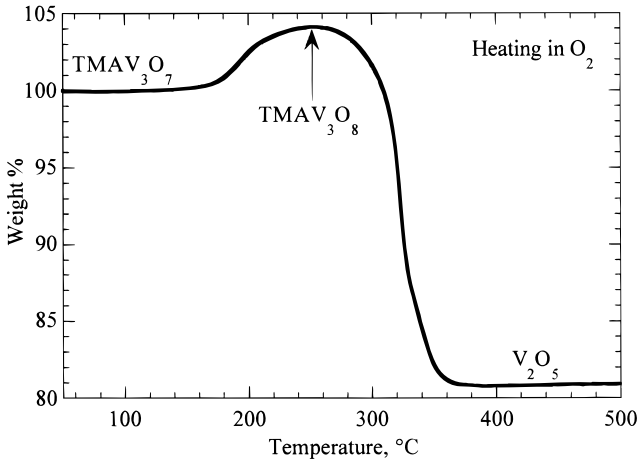

Figure 3. Thermal gravimetric analysis of $TMAV_3O_7$ in oxygen.

sharing tetrahedra. Each tetrahedron shares two corners with one square pyramidal chain, and one of the other two with the neighboring chain; the fourth oxygen is nonbonding and forms a vanadyl group. Which of these two oxygens is bonding has a significant impact on the planarity of the V_6O_{14} sheet. Thus, in $TMAV_3O_7$, the bonding leads to almost planar sheets,[27,38] as indicated in Figure 4. Similar planar sheets are found[39] in the two compounds $Zn(en)_2V_6O_{14}$ and $Cu(en)_2V_6O_{14}$, where the zinc and copper are six coordinate with two ethylenediamine molecules forming a square and two vanadyl oxygens providing the apical bonds. However, when the organic molecule can form hydrogen bonds, such as in MAV_3O_7[31,32] and $(DABCO)V_6O_{14}\cdot H_2O$,[36,37] the other oxygen in the VO_4 tetrahedron bonds to the adjoining chain, leading to a significant puckering of the vanadium sheets. This results in a reduction of the interchain distance from 8.427 Å in $TMAV_3O_7$ to 7.597 Å in MAV_3O_7; this tilting allows the vanadyl oxygens to come closer together, allowing hydrogen bonding to the MA or DABCO ions. A second distinguishing feature between the layers is the relative orientation of the neighboring chains. In the case of $DABCOV_6O_{14}$ and $TMAV_3O_7$, the chains are transformed into each other by a simple translation in the direction perpendicular to the chain, so that the repeat distance is simply equal to the distance between the chains. The transformation between the chains is more complex for MAV_3O_7 and $Zn(en)_2V_6O_{14}$ where the chains interact by a glide plane perpendicular to the chain. The relation between the structures formed by these four compounds is given in Table 2 (from Chen et al.[31]). A more complex situation is found[40] for $Ni(en)_2V_6O_{14}$, where there is marked order−disorder stacking of the vanadium oxide layers. This compound was made by the reaction of nickel sulfate, V_2O_5, and ethylenediamine in H_2O; the pH changed from 7.49 to 10 during the reaction. Interestingly, the magnetic behavior of the two planar compounds, $TMAV_3O_7$[29] and $Zn(en)_2V_6O_{14}$,[39] although complex and not yet understood, is the same but differs from that of the puckered $(DABCO)V_6O_{14}\cdot H_2O$.[37]

The electrochemical reduction of this structure type has been investigated in lithium cells. $TMAV_3O_7$ reacts with only 0.1 Li per formula unit; however, after oxidation to $TMAV_3O_8$ the lithium uptake increases substantially to a cutoff voltage of 2 V as shown in Figure 5. The DABCO V_6O_{14} phase reacted[36] with just 0.9 Li per formula unit, that is 0.15 Li/V to a cutoff of

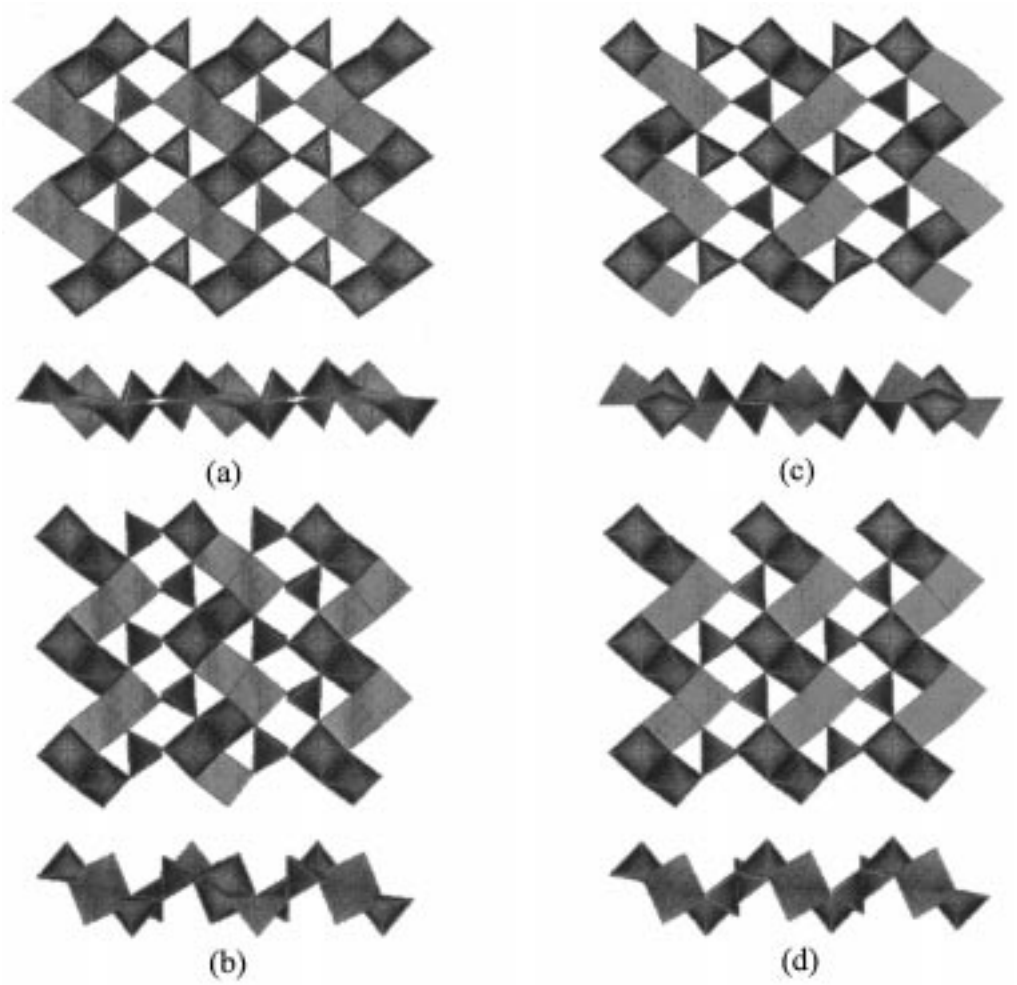

Figure 4. Structures of (a) $TMAV_3O_7$, (b) $CH_3NH_3V_3O_7$, (c) $en_2ZnV_6O_{14}$, or $en_2CuV_6O_{14}$, and (d) $(DABCO)V_6O_{14}\cdot H_2O$.

Table 2. Relation between the Four V_3O_7 Structures

symmetry relations between SP_2T chains	corner of tetrahedron shared between chains: top (→tilted layer)	corner of tetrahedron shared between chains: bottom (→flat layer)
glide plane	$(CH_3NH_3)V_3O_7$ t = 7.597 Å, c = 2t	$(en_2M)V_6O_{14}$ t = 7.851 Å, c = 2t
translation	$DABCOV_6O_{14}\cdot H_2O$ t = 7.574 Å, c = t	$TMAV_3O_7$ t = 8.427 Å, c = t

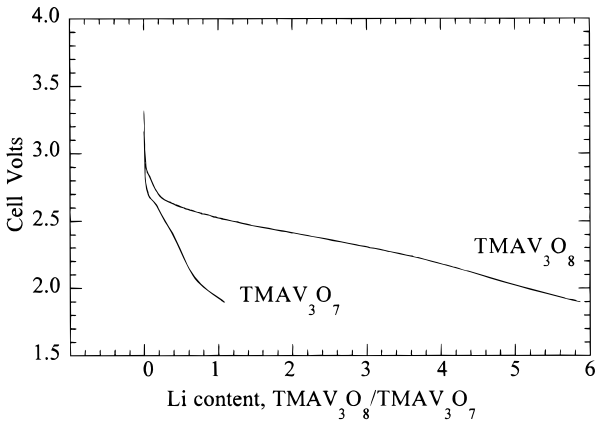

Figure 5. Electrochemical discharge of $TMAV_3O_7$ and $TMAV_3O_8$ normalized to $TMAV_3O_7$.

1.9 V. However, when the DABCO was removed by calcination at 400 °C, leading to a reduced vanadium oxide, $V_2O_{5-\delta}$, the reactivity increased to over 1Li/V and showed the stepwise discharge behavior typical of V_2O_5. When discharged to 1.9 V, the steps disappear and a single continuous discharge curve is obtained, similar to that of ω-V_2O_5.

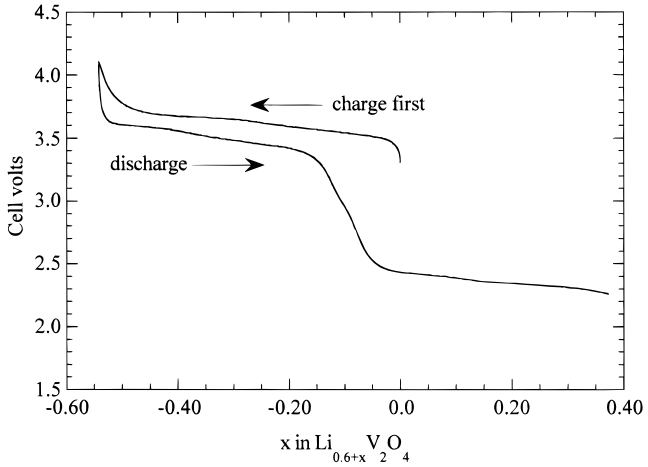

Figure 6. Electrochemical removal of lithium from $Li_xV_2O_4$, and subsequent reinsertion.

Vanadium Dioxide. When the pH of the reaction medium is reduced to around 5, a layered compound of formula $Li_xV_{2-\delta}O_{4-\delta}\cdot H_2O$ is formed[41] that contains no TMA ions. The water is reversibly lost on heating, leading to $Li_xV_{2-\delta}O_{4-\delta}$,[42] and the lithium can be readily and quantitatively removed in an electrochemical cell

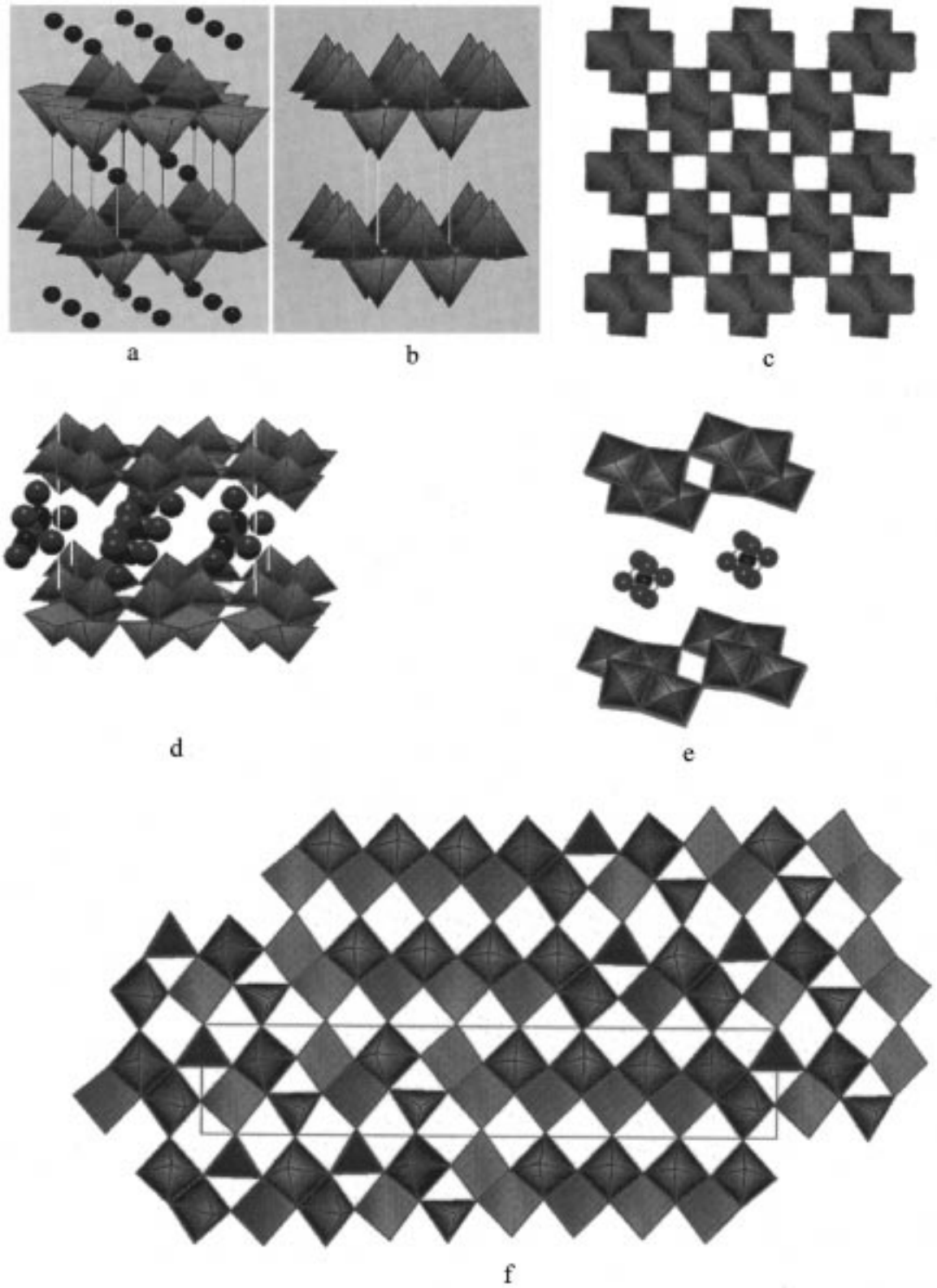

Figure 7. Structures of (a) $Li_xV_{2-d}O_{2-\delta}\cdot nH_2O$, (b) $Li_xV_{2-d}O_{2-\delta}$, (c) VO_2(B), (d) $TMAV_4O_{10}$, (e) $TMAV_8O_{20}$, and (f) $TMA_5V_{18}O_{46}$.

as shown in Figure 6, giving a new form of vanadium dioxide. The layer structure of this dioxide is closely related to that of vanadium pentoxide. The layer is constructed by corner sharing of VO_5 SPs, where the vanadyl apices alternate up and down as shown in Figure 7; water molecules and lithium ions reside between the layers. In V_2O_5 itself one-third of these SPs are missing in an ordered manner, leading to rows of vanadyl groups in the sequence -up-down-vacant-down-up-vacant-up-, whereas in VO_2 it is -up-down-up-down-. In $Li_xV_2O_4\cdot H_2O$ the vanadyl groups are directly above one another; when the water is removed the layers translate by half the unit cell along [110] to give the stacking sequence - - -V═O- - -V═O- - - with alternating long and short bonds as in V_2O_5. A neutron diffraction study showed that some of the lithium was located at

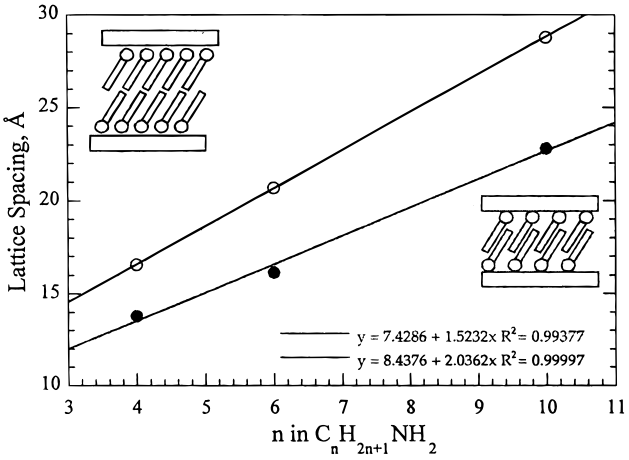

Figure 8. Intercalation of alkylamines into Li_xVO_2.

the vanadium vacancies, which is consistent with the known Li−O distances found in vanadium oxides such as $Li_xV_6O_{13}$[43] or Mg−O distances in $MgVO_3$.[44] A similar $VO_2 \cdot nH_2O$ without any lithium has been recently reported[45] by the reaction of hydrolyzed VCl_4 and 2.5 M NaOH at 200 °C for 92 h. The structure is the same as that of $Li_xV_2O_4 \cdot H_2O$.[33]

This vanadium oxide readily undergoes a variety of intercalation and ion-exchange reactions. Thus, a second layer of water can be intercalated, expanding the lattice to 10.9 Å. Alkylamines may also be intercalated, much as in the layered disulfides and oxides, leading to both single and double organic configurations as shown in Figure 8.

Figure 6 shows the electrochemical deintercalation of the dehydrated $Li_xV_2O_4$ and its subsequent reinsertion. This cycling of lithium appears to be totally reversible. When in the electrochemical cell the lithium content is first increased by discharging a $Li/Li_xV_2O_4$ cathode, an additional 1.4 lithium may be incorporated above 2 V. Extended cycling leads to single-phase behavior typical of ω-V_2O_5.[46]

Two other vanadium dioxides have been synthesized hydrothermally, VO_2(A) and VO_2(B). VO_2(B) is formed[47] by reacting a mixture of V_2O_5, V_2O_3, and water at 200 °C. On heating VO_2(B) hydrothermally above 220 °C, it converts to VO_2(A), and on further heating, ≈350 °C, the stable rutile form of VO_2 is obtained. VO_2(B) has a shear-type structure that is related topotaxially[47] to that of V_6O_{13}; the latter's structure is built from alternating single and double sheets of vanadium oxide, −S-D−S-D−S, whereas VO_2(B) has only double layers. Oka et al.[48] made VO_2(A) by the hydrothermal treatment of an aqueous suspension of $VO(OH)_2$ at 250 °C for 48 h, and found that its structure differs from that of VO_2(B) only in the stacking of the VO_6 sheets. Thus both of these dioxides have a three-dimensional (3D) structure that consists of VO_6 octahedra. VO_2(A) appears to undergo a phase transition at 162 °C similar to that of the rutile form,[49] indicating vanadium−vanadium pairing.

The B form has been studied[50] in electrochemical cells and found to readily intercalate lithium with a limiting stoichiometry of $Li_{0.5}VO_2$, that is, slightly less than for $Li_xV_{2-\delta}O_{4-\delta}$.[42] In contrast, the rutile form is essentially inactive, with ≤0.1 Li incorporated.[51−53] This might be related to the relative openness of the structures; the rutile form has a density of 4.657 g/cm^3, the A and B forms 4.035 and 4.031 g/cm^3, respectively, and $Li_xV_2O_4$ 3.11 g/cm^3.

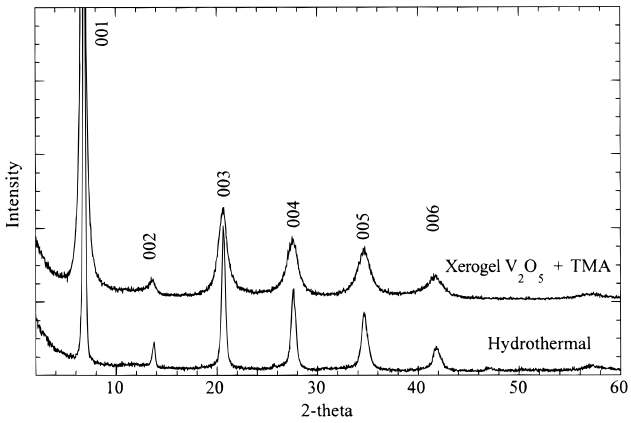

Figure 9. X-ray diffraction pattern of $TMA_{0.17}H_{0.1}V_2O_5$ compared with that of xerogel V_2O_5 reacted with TMA.

Other TMA Compounds

$TMAV_4O_{10}$ was the first organic layered compound of vanadium oxide to be formed hydrothermally;[33] the structure, shown in Figure 7, contains only VO_5 SPs.[30,54] These pyramids have the same chain arrangement as in V_2O_5 and NaV_2O_5; however, whereas in V_2O_5 the adjoining edge-sharing pyramids alternate their apices up and down, in $TMAV_4O_{10}$ they are arranged in pairs two up and then two down along the edge-sharing chain.

The fettucini-like morphology of the $TMAV_8O_{20}$ phase is an indication of the strong bonding in one dimension, and the structure bears this out. This compound[28] is built from a common building block in the vanadium oxides—a quadruple unit of edge-sharing vanadium octahedra. These form chains down the *b* axis, and they join together forming the V_8O_{20} sheets by sharing two corners, as indicated in Figure 7. The large TMA cations, of diameter ca. 7 Å, are arranged in a disordered manner around the 0,0,0 site, thus explaining the small *b* axis of 3.59 Å. Removal of the TMA ions results in destruction of the lattice.

The $TMA_{0.17}H_{0.1}V_2O_5$ phase, formed under the most acidic conditions, has an interlayer spacing of 12.97 Å, and appears to be very similar to the xerogel V_2O_5 formed by acidification of vanadates at room temperature. Figure 9 compares[29] the X-ray diffraction of the hydrothermally formed phase with a xerogel, $H_xV_2O_5 \cdot nH_2O$, that has been reacted with the base TMAOH. The two phases are clearly similar, with the hydrothermal phase being the more crystalline; we are hoping to be able to get a better understanding of the structure of this phase by studying this more crystalline phase. Oka et al.[55] have proposed that the structure of V_2O_5 xerogel is based on that of δ-V_2O_5. The layers of δ-V_2O_5 are built from a quadruple unit of edge-sharing vanadium octahedra. The quadruple unit forms the chain by sharing an edge with the neighboring units. The cations, water, or both reside between the vanadium layers.

The layered $TMA_5V_{18}O_{46}$ is found[56] as a minor component when V_2O_5, V_2O_3, TMACl, and TMAOH in the molar ratio 1:0.33:1:5 are heated at 170 °C for 2 days after adjustment of the pH to 5.0 with nitric acid. The major components were $TMAV_4O_{10}$ (40%) and the

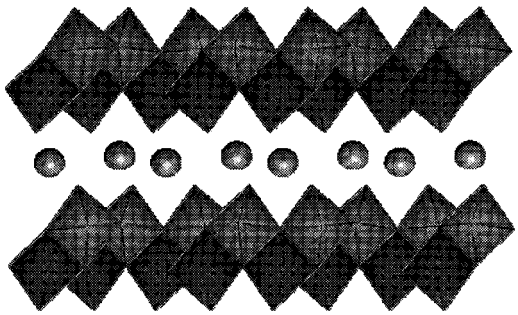

Figure 10. The δ-V_2O_5 structure of $(CH_3NH_3)_{0.75}V_4O_{10}\cdot H_2O$.

cluster compound $TMA_6V_{15}O_{36}Cl\cdot 4H_2O$ (40%). It has a unique intergrowth structure, shown in Figure 7, whose unit cell is comprised of two distinct slabs ≈12 Å wide and 7 Å thick. The slabs have very different vanadium coordination environments; this results in the slabs being either slightly curved and neutrally charged or puckered with negative charges (counterions are TMA).

Methylamine Compounds

When methylamine is substituted for the TMA ion, the opportunity for hydrogen bonding is made available and indeed some differences in reactivity and crystalline structure are found. However, pH is still important in determining the structure formed, with three compounds formed to date. When a mixture of V_2O_5 and CH_3NH_2, with the pH adjusted to 7 with acetic acid, is reacted at 200 °C for 4−5 days, large, dark-brown platelike crystals of $(CH_3NH_3)V_3O_7$ are formed;[31] the pH of the reaction remained constant during the reaction. The structure of $(CH_3NH_3)V_3O_7$ was shown in Figure 4. The MA cations reside between the layers and are bonded to the oxygens of the vanadium layers, which are puckered as in $(DABCO)V_6O_{14}\cdot H_2O$. The methylamine was lost on heating in oxygen between 200 °C and 280 °C with the formation of vanadium pentoxide.

Lowering the pH of the V_2O_5-methylamine system to 4 with acetic acid resulted in the formation of dark-green claylike $(CH_3NH_3)_{0.75}V_4O_{10}\cdot H_2O$.[31] The inorganic framework of this compound is built from double V_2O_5 layers, shown in Figure 10, like those in δ-V_2O_5 and xerogel V_2O_5. The MA cation resides between the vanadium oxide layers. The TGA showed the loss of organic between 200 °C and 300 °C and formation of V_2O_5.

Changing the pH of the V_2O_5-methylamine system to 3.5 with a mineral acid, HNO_3, resulted in the formation of $(CH_3NH_2)_2V_8O_{17}$.[32] The pH jumps to 9 after the reaction and shiny black crystals were the product of the reaction; the same product is formed in the absence of acid addition. The composition of this compound was determined by chemical analysis. The compound loses the organic at 300 °C, followed by the gain of oxygen to form V_2O_5. The structure of this compound has not yet been solved.

Bidentate Organic Complexes

A number of bidentate organic molecules such as ethylenediamine, $H_2NCH_2CH_2NH_2$ = en, diaminopropane, $NH_2CH_2CH_2CH_2NH_2$, and piperazine, $HN(C_2H_4)_2NH$, have been shown to form layered vanadium oxide

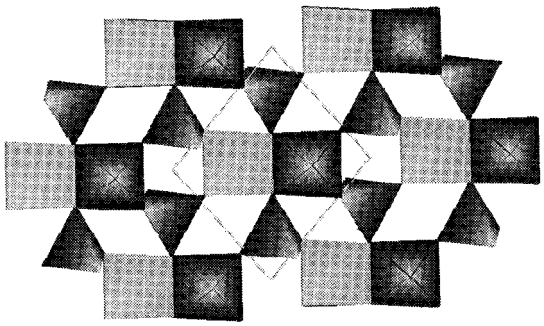

Figure 11. Structure of vanadium oxide layer in α-and β-$(H_3NCH_2CH_2NH_3)V_4O_{10}$.

compounds. The pH of most of the reaction media is neutral to basic after reaction, consistent with the structures found that contain both SPs and tetrahedra; the vanadium oxidation state is between +4 and +5. Riou and Férey[57] made green crystals of $(enH_2)V_4O_{10}$ by the hydrothermal treatment of the reaction mixture, V_2O_5, SiO_2, HF, en and H_2O at 180 °C for 24 h. The pH of the reaction medium changed from 5 to 7 during the reaction. Zhang et al. reported[58] black and rod-shaped α- and β forms of this compound when V_2O_5, en and H_2O were reacted at 180 °C for 121 h, and they were always found together. The unit cell of the α-$(H_3NCH_2CH_2NH_3)_{0.5}V_2O_5$ is different from the β form because of the orientation of the ethylenediamine between the vanadium layers. In the α form, the enH_2 cations lie parallel to the layers, whereas in the β form these cations are oriented with a small tilt angle, which results in slight puckering of the vanadium oxide sheets for the β form. This leads to a larger interlayer spacing of 7.246 Å for the β form, compared with 7.187 Å for the α form. The inorganic framework is the same for both forms, as shown in Figure 11, and is composed of vanadium oxide layers with the formula $V_2O_5^-$ and consists of both V^VO_4 tetrahedra and $V^{IV}O_5$ square pyramids. Two SPs share edges and their terminal oxygens are oriented in opposite directions. The pair of SPs are linked to 6 VO_4 units. This type of building unit has been previously observed in the structure of CsV_2O_5.[59] The major difference is the orientation of the tetrahedra in both compounds. In CsV_2O_5, the terminal oxygen of the tetrahedron points up and down alternatively from row to row. The VO_4 units in $(enH_2)V_4O_{10}$ alternatively point up and down in each row toward the organic layer.

Riou and Férey[60] synthesized a diaminopropane analogue under slightly more acidic conditions, initial pH 4 and final 5; $[H_3N(CH_2)_3NH_3]V_4O_{10}$ was formed as dark-green hexagonal plates. Zhang et al.[61] reported finding black platelike crystals. The inorganic framework of this compound is the same as that of (enH_2)-V_4O_{10}, except that it differs in the way the layers are packed. Every other layer of SPs is shifted by a/2 differing with the structure of $(enH_2)V_4O_{10}$. The shift in the SP layers results in a larger unit cell (Table 1). The diprotonated diaminopropane resides between the vanadium sheets and lies parallel to the layers and hydrogen bonds to oxygens in the vanadium layers.

Piperazine behaves similarly to ethylenediamine, and Riou and Férey[57] made green crystals of α-$(pip)V_4O_{10}$ under the same reaction conditions, with the pH again

changing from 5 to 7 upon completion of the reaction. The structure of this compound is the same as that of $(en)V_4O_{10}$ except that the interlayer spacing is larger in $(pip)V_4O_{10}$ because of the presence of the larger piperazine cations between the vanadium layers, 8.20 Å vs. 7.47 Å.

Zhang et al.[58] synthesized α- and β-$(pip)V_4O_{10}$ compounds as thin black plates from the hydrothermal treatment of the reaction mixture $NaVO_3$, $H_2O_3PCH_3$, piperazine, and H_2O at a pH of 7. The structure of β-$(pip)V_4O_{10}$ is different from that of α-$(pip)V_4O_{10}$ and enV_4O_{10}. The vanadium layers are made from both SPs and tetrahedra. The SPs exist in pairs sharing their edges, similar to the stacking seen in $(enH_2)V_4O_{10}$. The difference in the structure is due to the arrangement of the SPs. Two different orientations are observed from one SP row to the next. The piperazinium cations residing between the layers are hydrogen bonded to the layer oxygens in both α- and β-$[H_2N(C_2H_4)_2NH_2]V_4O_{10}$.

Zinc Vanadium Oxides

So far we have predominantly discussed reactions where only one metal, vanadium, or lithium and vanadium were present. The impact of a second metal, in particular zinc, in the reaction medium has been extensively studied both with organics such as TMA, en and bypyridine present and absent.

The hydrothermal treatment of the reaction mixture V_2O_5, ZnO, H_2O, and bpy in the molar ratios of 1:0.35:323:1.2 at 170 °C for 44 h followed by 200 °C for 90 h resulted in black rods of $[(bpy)_2Zn]_2V_4O_{10}$.[39] In contrast to the compounds described so far, the inorganic framework of the layers is built only from tetrahedra. The oxidation state of vanadium is thus in the +5 state. Each tetrahedra shares three of its corners and has a terminal oxygen. Fourteen VO_4 tetrahedra make up large circular rings in each layer. The $Zn(bpy)_2$ complex is on either side of the center of the ring bonded to the oxygens of the vanadium layers.

When $VO(OH)_2$ and a 0.1 M $ZnCl_2$ solution are heated at 280 °C for 40 h, a black powder of composition σ-$Zn_{0.25}V_2O_5{\cdot}H_2O$ with a new type of V_2O_5 layer was formed.[62] Its layered structure contains vanadium oxide tetrahedra, SPs, and octahedra. This structure when projected in the ab plane is similar to that of δ-V_2O_5. The Zn and the water molecules are located between the layers. This phase can be dehydrated by heating the sample to 200 °C. The layer spacing decreases from 10.76 Å to 8.92 Å upon removal of the water.

A systematic study[63] of the reaction of $ZnCl_2$, V_2O_5, and TMAOH with varying molar ratios of 1:1:1, 1:1:2, 1:1:3, and 1:1:4 resulted in the formation of four new phases, $Zn_{0.4}V_2O_5{\cdot}0.3H_2O$, $Zn_{0.4}V_2O_5{\cdot}0.5TMA$, $Zn_3(OH)_2(V_2O_7){\cdot}H_2O$, and $Zn_2(OH)_3(VO_3)$, respectively. When $Zn_{0.4}V_2O_5{\cdot}0.5TMA$ was synthesized, the pH was adjusted to 3.67−4.00 by acetic acid. The colors of these four compounds are greenish black, black, white, and white, respectively. Two of these compounds, $Zn_{0.4}V_2O_5{\cdot}0.3H_2O$ and $Zn_{0.4}V_2O_5{\cdot}0.5TMA$, as well as a similar iron compound $TMA_{0.17}Fe_{0.1}V_2O_5{\cdot}0.17H_2O$,[64] contain vanadium oxide in double sheets as in δ-V_2O_5[65] (see Figure 10). $Zn_{0.4}V_2O_5{\cdot}0.3H_2O$ has a repeat distance of 10.43 Å, consistent with a double layer sheet of V_2O_5 with zinc ions and water molecules between the layers. On heating to 150 °C, the lattice contracted from 10.43 to 9.23 Å; on exposure to atmospheric air, the lattice expanded again to 10.48 Å and 10.59 Å, indicating a variable water content. This δ phase has also been formed by the hydrothermal treatment of the $VOSO_4$−$ZnSO_4$ system or the $VO(OH_2)$−$ZnCl_2$ system at 250−280 °C,[62] but the higher temperature leads to a lower zinc content, δ-$Zn_{0.16}V_2O_5{\cdot}nH_2O$. It is also formed by the ion exchange of $(VO)_{0.1}V_2O_5{\cdot}nH_2O$ or $K_{0.3}V_2O_5$ in $ZnCl_2$ solution. The ion-exchange activity is higher for the δ-phase than that of the σ-phase, σ-$Zn_{0.25}V_2O_5{\cdot}H_2O$. The water content is variable and the interlayer spacing ranges from 13.15 Å at room temperature to 9.31 Å at 180 °C.

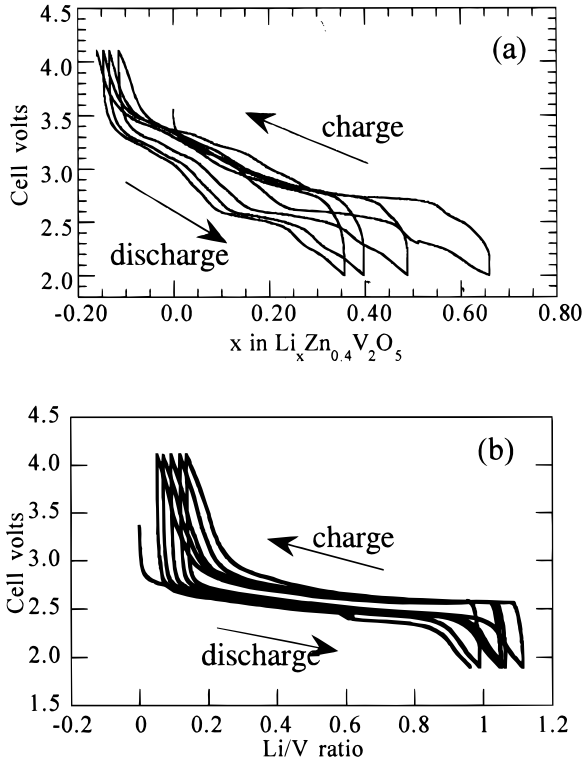

Figure 12. Electrochemical insertion of lithium into (a) $Zn_{0.4}V_2O_5{\cdot}0.3H_2O$ and (b) $Zn_{0.4}V_2O_5{\cdot}0.5TMA$.

The electrochemical behavior of the δ-V_2O_5 zinc vanadium oxides is shown in Figure 12.[63,64] The lithium insertion proceeds in several stages, reminiscent of that of V_2O_5. These steps are maintained during the subsequent charge and discharge cycles, showing that the structure of this material did not change during the redox reactions, unlike V_2O_5 itself. The lattice repeat distance of dehydrated $Zn_{0.4}V_2O_5{\cdot}0.3H_2O$ decreases to 8.62 Å when reacted with *n*-butyllithium in hexane. The compound $Zn_{0.4}V_2O_5{\cdot}0.5TMA$ incorporates 1.1 lithium into the structure on discharge, consistent with the vanadium being reduced to the +4 oxidation state. In this case the discharge curve does not show the steps observed in the TMA free compound.

The third compound formed, $Zn_3(OH)_2V_2O_7{\cdot}2H_2O$, is a pillar compound reminiscent of β-alumina. The structure is sandwich-like (Figure 13),[66] with the layers comprising zinc oxide/hydroxide octahedra, with V_2O_7 groups making V−O−V pillars and water molecules between the layers. The water is readily and reversibly removed on heating; less than half the volume between the layers is occupied in the dehydrated compound. This

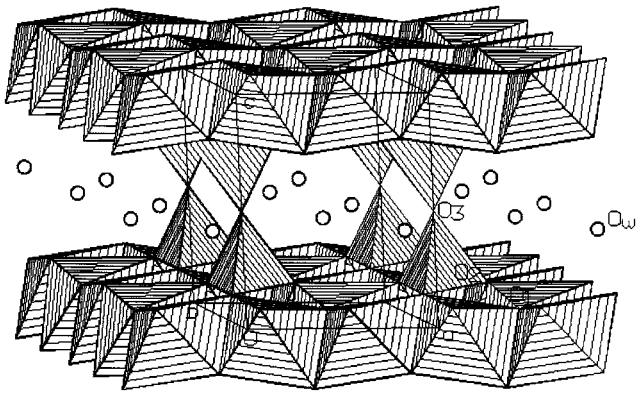

Figure 13. The structure of $Zn_3(OH)_2V_2O_7 \cdot 2H_2O$, open circles are water molecules.

void space should lead to high diffusivity of ions or molecules that can fit between the layers. The challenge is now to duplicate the structure with a more interesting and redox-active ion than zinc in the layers.

The fourth compound formed, $Zn_2(OH)_3(VO_3)$, was indexed in space group R-3m with hexagonal lattice parameters: $a = 3.0721(1)$ Å, $c = 14.313(3)$ Å.[63] This compound has layers of edge-shared zinc oxide/hydroxide octahedra, with vanadium between the layers in tetrahedral configuration. The layers can be thought of as having the composition $H_3(Zn_2\square)O_6$, where Zn occupies two of the three available octahedral sites, and is the vacancy. This compound is essentially inactive to lithium in electrochemical cells, probably because of its close-packed structure.

The $en_2ZnV_6O_{14}$ and $en_2CuV_6O_{14}$ compounds with the V_3O_7 type structure were described above. When the reaction molar ratios were changed, a new compound, $[(en)_2Cu]_2[V_{10}O_{25}]$,[39] resulted, with copper chelated to en between the layers. The layers contain vanadium SPs and tetrahedra. The SPs share edges and form a trimeric unit. In the trimeric unit, two SPs face up and one faces down. The trimeric unit shares it corners along the [001] direction to form chains. Two of the chains join together by the tetrahedra to form a double strand. These double strands are joined by a V_2O_7 pair of tetrahedra and create some ordered voids in the layers.

Structures with V_3O_8 Layers

$H_2V_3O_8$ or $V_3O_7 \cdot H_2O$ was originally synthesized by Theobald and Cabala[67] and its structure solved by Oka et al.[68] Green flat fibers of $H_2V_3O_8$ were prepared by the hydrothermal treatment of $VOSO_4$ aqueous solution at 0.1−0.2 M. It can also be synthesized[69,70] by the hydrothermal reaction at 200 °C of V_2O_5 in glacial acetic acid to which a little water has been added. The structure of this compound is shown in Figure 14, and contains vanadium SPs and octahedra in +4 and +5 oxidation states, respectively. Four vanadium octahedra shares edges, forming a quadruple unit. The two SPs with terminal oxygens facing in the opposite direction are joined by sharing an edge at the base. The SP units bridge the quadruple units to form the layers. The water is bound to the vanadium in place of one of the oxygens in the VO_6 octahedron and makes hydrogen bonds with the octahedra in the next layer, giving the 3D structure.

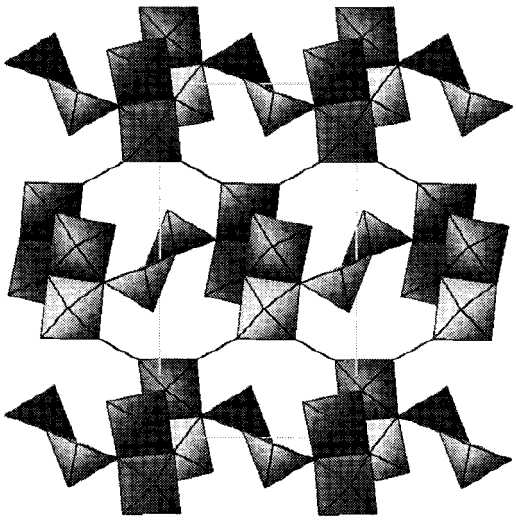

Figure 14. Structure of $H_2V_3O_8$.

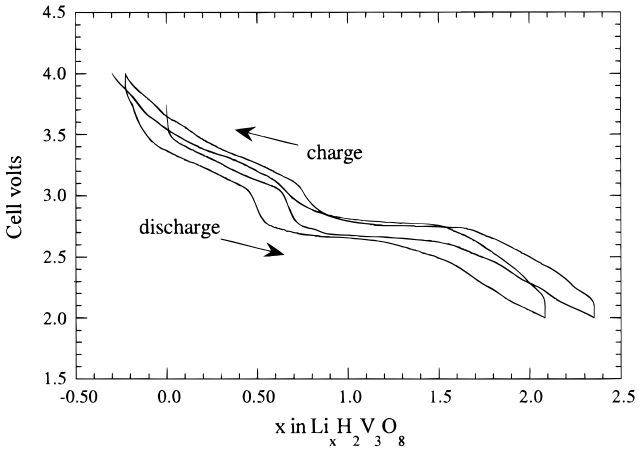

Figure 15. Electrochemcial insertion of lithium into $H_2V_3O_8$.

The magnetic susceptibility of $H_2V_3O_8$ exhibits Curie−Weiss behavior and is consistent with one isolated V^{IV} per formula unit.[69] This compound also exhibits interesting electrochemical behavior in lithium cells, as shown in Figure 15.[71] The plateaus indicate that the lithium is residing in several different sites, and that the reactions are reversible.

Oka et al.[72] synthesized the known compounds AV_3O_8 (A = K, Rb, and Cs) by the hydrothermal treatment of V_2O_5 and ANO_3 solutions at 250 °C for 48 h, and showed that RbV_3O_8 has the known structure of the KV_3O_8 and CsV_3O_8 compounds.[73] The V_3O_8 layer is made of VO_6 octahedra and V_2O_8 units of edge-sharing SPs. The alkali ions are situated between the layers. $NH_4V_3O_8$ was also synthesized and had the structure described by Range et al.[74] Attempts to make LiV_3O_8 and NaV_3O_8 hydrothermally were unsuccessful. The reactants and synthesis conditions were critical in forming, with nitrate maintaining the highest vanadium oxidation state. The $V_2O_5-A_2SO_4$ system produced $A_2V_6O_{16} \cdot nH_2O$ compounds related to the hewettite mineral, $CaV_6O_{16} \cdot nH_2O$.[75]

Barium Vanadium Oxides

Several barium vanadium oxides have been formed hydrothermally.[76−78] The hydrothermal reaction of $VO(OH)_2$ dispersed in a 0.1 M $BaCl_2$ solution at 270 °C for

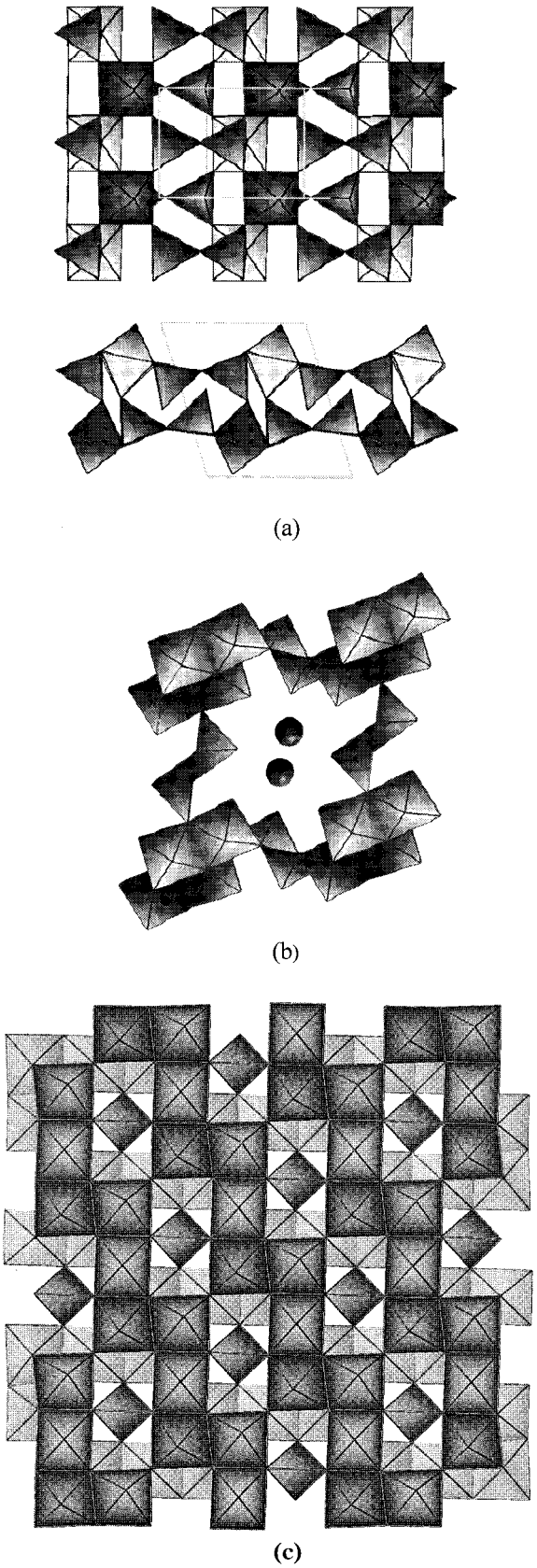

Figure 16. The structure of barium vanadium oxides: (a) BaV_3O_8, (b) $Ba_{0.4}V_3O_8(VO)_{0.4}\cdot 0.4H_2O$, and (c) $BaV_7O_{16}\cdot nH_2O$.

40 h resulted in the formation of black rodlike crystals of BaV_3O_8[76] together with VO_2(A). This compound was first reported by Bouloux et al.[79] to be $Ba_{1+y}(V_3O_8)_2$, but the structural details were unknown. The layered structure of BaV_3O_8, shown in Figure 16a, is of V_3O_8 layers stacked along the *c*-axis. The V_3O_8 framework is made of vanadium tetrahedra and octahedra. Two vanadium tetrahedra share a corner to form a V_2O_7 unit. This V_2O_7 units shares its vertices with VO_6 octahedra to form a V_3O_9 sheet. The two V_3O_9 sheets are connected at octahedra of one sheet to the tetrahedra of the other sheet making up the V_3O_8 layer. The barium ions are found between the V_3O_8 layers.

$Ba_{0.4}V_3O_8(VO)_{0.4}\cdot 0.4H_2O$ was synthesized by the hydrothermal reaction of $VOCl_2$ and $BaCl_2$ at 240 °C for 24 h.[78] The vanadium is present in both +4 and +5 oxidation states. The V_3O_8 layer is the same as that of $H_2V_3O_8$, with the vanadium in square pyramidal and octahedral coordination, but instead of the hydrogen bonds that connect the layer, the V_3O_8 layers are bridged by vanadyl groups forming VO_5 SPs (Figure 16b). The bridging, however, is imperfect, as 60% of the VO_5 units are absent and thus the structure of $Ba_{0.4}V_3O_8(VO)_{0.4}\cdot 0.4H_2O$ is intermediate between a tunnel and layer structure. The barium ions and the water molecules are located in the tunnels; potassium and rubidium form analogous compounds.

Jacobson and colleagues[80] synthesized a new barium vanadium oxide, $BaV_7O_{16}\cdot nH_2O$, using the electrochemical−hydrothermal method of Yoshimura et al.[81] Its structure, which has tetragonal symmetry, bears some similarities to the V_6O_{14} structure type discussed earlier, as it contains zigzag chains of edge-sharing polyhedra, as shown in Figure 16c;[80] in this case VO_6-distorted octahedra, where the former contains VO_5 SPs. These chains are joined by corner-sharing to give sheets with all the vanadyl groups on one side; two such sheets are then joined back to back to make the vanadium oxide layer. Tetrahedra are located between the 1 × 2 windows of both structures, and all four oxygens are shared with the layers. It thus has similarities to both δ-$Zn_{0.40}V_2O_5\cdot nH_2O$[64] and σ-$Zn_{0.25}V_2O_5\cdot H_2O$.[62]

δ-V_2O_5-Type Structures

Oka et al.[82] made a systematic study of the hydrothermal reaction of $VOSO_4$ solutions in an attempt to synthesize layered compounds similar to the V_2O_5 gels, and identified five phases as a function of $VOSO_4$ concentration and reaction temperature. The major phase, designated as I, has a temperature-dependent interlayer spacing: 14.3 Å at 240 °C and 17.3 Å at 170 °C. Heating or evacuation gives a series of compounds: I′ (17.3 Å)→I (14.2 Å)→Iα′ (12.6 Å)→ Iα (11.5 Å)→Iβ (10.0 Å)→Iγ (8.3 Å); phases I through Iβ transitions are reversible. Phase I has the composition[83] $(VO)_{0.1}V_2O_5\cdot 2.3H_2O$. The vanadyl ions ($VO^{2+}$) and water molecules are intercalated between the V_2O_5 layers, which are similar to the double sheets of δ-V_2O_5. This phase is similar to the V_2O_5 gel product, reported by Babonneau et al.[84] and Khairy et al.,[85] which has an interlayer spacing of 14.2 Å, as does the hydrothermally formed compound $V_2O_{4.8}\cdot 0.5H_2O$ reported by Theobald and Cabala.[86,87] Phase I is very similar to the mineral bariandite,[88] $V_{10}O_{24}\cdot 12H_2O$, which has the same lattice parameters and is likely isostructural.

Phase II was formed at higher temperatures, > 250 °C, has an interlayer spacing of 8.3 Å, and was found[89] to be an aluminum-containing oxide, $(V_{1-x}Al_x)_2O_{5-4x}$-

$(OH)_{4x}$, with $x = 0.18$. The aluminum was believed to come from the reaction vessel. The layers of phase II are also analogous to the δ-V_2O_5 structure. Phases III and IV were formed at still higher temperatures and have interlayer spacings of 19.0 Å and 7.1 Å. Phase V was formed at higher $VOSO_4$ concentrations along with phase I and $V_3O_7 \cdot H_2O$ at temperatures >250 °C with an interlayer spacing of 13.2 Å.

The addition of alkali ions and NH_4 ions to the $VOSO_4$ reaction solutions results in hydrated layered structures with the general composition $A_{0.3}V_2O_5 \cdot nH_2O$ (A = Na, K, Rb, Cs, NH_4 and n = 0.6−1.2).[90,91] The interlayer spacing for these compounds is ≈11 Å, which is reduced on dehydration to values dependent on the size of the alkali ions; reversion to the hydrated form occurs upon exposure to air. When the alkali content is increased, as in $K_{0.5}V_2O_5$[92] and $Rb_{0.25}V_2O_5$,[93] the compounds remain anhydrous and have the δ-V_2O_5-type structure. When the potassium content is between 0.29 and 0.33 the hydrated form results, and when it is between 0.46 and 0.50, the dehydrated form is observed. A biphasic state is observed when the potassium content is between 0.33 and 0.46. The layer spacing of the hydrated form is 10.88 Å, which decreases to 9.5 Å upon the removal of water. The increased potassium content binds the V_2O_5 layers together strongly enough so the layers cannot expand and allow the water molecules to intercalate between the layers. The $K_{0.5}V_2O_5$ phase can be hydrated by oxidative removal of potassium in 3% hydrogen peroxide solution; addition of K from a KI solution adds potassium and removes the water. The $Rb_{0.5}V_2O_5$ phase can also be oxidized and hydrated to $Rb_{0.3}V_2O_5 \cdot 0.8H_2O$ by soaking in hydrogen peroxide solution; however, subsequent reduction of the hydrated phase in RbI solution only results in a less hydrated phase, $Rb_{0.4}V_2O_5 \cdot 0.5H_2O$.

Oka et al.[94] were also successful in the hydrothermal synthesis, from VO_2(A) and MCl_2 solutions, of single crystals of $M_{0.25}V_2O_5 \cdot H_2O$, where M = Ca or Ni. They showed that these compounds have the δ-V_2O_5 structure with Ca or Ni and the water molecules residing between the layers.

Aluminum Vanadium Oxide

Pequenard et al.[95] showed that reaction of aluminum and vanadium oxides under hydrothermal conditions, using TMA ion as a template, gives rise to a new aluminum vanadium oxide hydroxide $Al_2(OH)_3(VO_4)$, which has the structure of the mineral augelite $Al_2(PO_4)(OH)_3$.[96] This new compound, as well as augelite, is one of the few compounds to contain aluminum in a trigonal pyramidal environment.

Cesium Vanadium Oxide

Yellow crystals of $Cs_2V_4O_{11}$, first reported by Perraud,[97] were synthesized by the hydrothermal reaction of $VO(OH)_2$ and $CsVO_3$ in water at 280 °C for 30 h.[98] The structure is made of V_4O_{11} layers with the cesium ions residing between the layers, which contain VO_4 tetrahedra and VO_5 SPs in a random distribution.

Acknowledgment. We thank the Department of Energy through the Lawrence Berkeley Laboratory and the National Science Foundation through grant DMR-9422667 for partial support of this work. We also thank Professor Richard Naslund for the use of the DCP atomic emission spectrometer, and Bill Blackburn for the electron microprobe studies.

References

(1) Barrer, R. M. *Hydrothermal Chemistry of Zeolites*; Academic Press: London, 1982.
(2) Beck, J. S.; Vartuli, J. C.; Roth, W. J.; Leonowicz, M. E.; Kresge, C. T.; Schmitt, K. D.; Chu, C. T.-W.; Olson, D. H.; Sheppard, E. W.; McCullen, S. B.; Higgins, J. B.; Schlenker, J. L. *J. Am. Chem. Soc.* **1992**, *114*, 10834.
(3) Huo, Q. S.; Margolese, D. I.; Ciesla, U.; Feng, P.; Gier, T. E.; Sieger, P.; Leon, R.; Petroff, P. M.; Schuff, F.; Stucky, G. D. *Nature* **1994**, *368*, 317.
(4) Stein, A.; Fendorf, M.; Jarvie, T.; Mueller, K. T.; Benesi, A. J.; Mallouk, T. E. *Chem. Mater.* **1995**, *7*, 304.
(5) Whittingham, M. S.; Li, J.; Guo, J.; Zavalij, P. *Mater. Sci. Forum* **1994**, *99*, 152−153.
(6) Janauer, G. G.; Dobley, A.; Guo, J.; Zavalij, P.; Whittingham, M. S. *Chem. Mater.* **1996**, *8*, 2096.
(7) Janauer, G. G.; Zavalij, P. Y.; Whittingham, M. S. *Chem. Mater.* **1997**, *9*, 647.
(8) Luca, V.; MacLachlan, D. J.; Hook, J. M.; Withers, R. *Chem. Mater.* **1995**, *7*, 2220.
(9) Günter, J. R.; Amberg, M.; Schmalle, H. *Mater. Res. Bull.* **1989**, *24*, 289.
(10) Reis, K. P.; Ramanan, A.; Whittingham, M. S. *Chem. Mater.* **1990**, *2*, 219.
(11) Reis, K. P.; Whittingham, M. S. *J. Solid State Chem.* **1991**, *91*, 394.
(12) Reis, K. P.; Ramanan, A.; Gloffke, W.; Whittingham, M. S. In *Solid State Ionics II*; Nazri, C. A., Shriver, D. W., Huggins, R. A., Balkanski, M., Eds.; Materials Research Society: Boston, 1991; Vol. 210, p 473.
(13) Reis, K. P.; Ramanan, A.; Whittingham, M. S. *J. Solid State Chem.* **1992**, *96*, 31.
(14) Reis, K. P.; Prince, E.; Whittingham, M. S. *Chem. Mater.* **1992**, *4*, 307.
(15) Zavalij, P.; Guo, J.; Whittingham, M. S.; Jacobson, R. A.; Pecharsky, V.; Bucher, C.; Hwu, S.-J. *J. Solid State Chem.* **1996**, *123*, 83.
(16) Guo, J.; Li, Y. J.; Whittingham, M. S. *J. Power Sources* **1995**, *54*, 461.
(17) Guo, J.; Zavalij, P.; Whittingham, M. S. *Eur. J. Solid State Chem.* **1994**, *31*, 833.
(18) Guo, J.; Zavalij, P.; Whittingham, M. S. *Chem. Mater.* **1994**, *6*, 357.
(19) Livage, J. *Mater. Res. Bull.* **1991**, *26*, 1173.
(20) Livage, J. *Chem. Mater.* **1991**, *3*, 578.
(21) Livage, J.; Baffier, N.; Pereira-Ramos, J. P.; Davidson, P. *Mater. Res. Soc. Proc.* **1995**, *369*, 179.
(22) Livage, J. *Proc. Lake Louise Composites: Design for Perfomance*; Eagle Press, 1997; 45.
(23) Tarascon, J. M.; Wang, E.; Shokoohi, F. K.; McKinnon, W. R.; Colson, S. *J. Electrochem. Soc.* **1991**, *138*, 2859.
(24) Maingot, S.; Baddour, R.; Pereira-Ramos, J. P.; Baffier, N.; Willmann, P. *J. Electrochem. Soc.* **1993**, *140*, L158.
(25) Maingot, S.; Deniard, P.; Baffier, N.; Pereira-Ramos, J. P.; Kahn-Harari, A.; Brec, R. *Mater. Sci. Forum* **1994**, *297*, 152−153.
(26) Whittingham, M. S. Current Opinion in Solid State & Materials Science, **1996**, *1*, 227.
(27) Chirayil, T. A.; Zavalij, P. Y.; Whittingham, M. S. *J. Chem. Soc., Chem. Commun.* **1997**, 33.
(28) Chirayil, T.; Zavalij, P. Y.; Whittingham, M. S. *J. Mater. Chem.* **1997**, *7*, 2193.
(29) Chirayil, T. Ph.D. Thesis, State Univeristy of New York at Binghamton, 1998.
(30) Boylan, E. A.; Chirayil, T.; Hinz, J.; Zavalij, P.; Whittingham, M. S. *Solid State Ionics* **1996**, *90*, 1.
(31) Chen, R.; Zavalij, P. Y.; Whittingham, M. S.; Greedan, J. E.; Raju, N. P.; Bieringer, M. *J. Mater. Chem.* **1998**, *8*, in press.
(32) Chen, R.; Zavalij, P. Y.; Whittingham, M. S. *Mater. Res. Soc. Proc.* **1998**, *497*, in press.
(33) Whittingham, M. S.; Guo, J.; Chen, R.; Chirayil, T.; Janauer, G.; Zavalij, P. *Solid State Ionics* **1995**, *75*, 257.
(34) Chirayil, T.; Zavalij, P. Y.; Whittingham, M. S. *Acta Crystallogr.* **1998**, in press.
(35) Chirayil, T.; Zavalij, P. Y.; Whittingham, M. S. *Mater. Res. Soc. Proc.* **1997**, *453*, 135.
(36) Nazar, L. F.; Koene, B. E.; Britten, J. F. *Chem. Mater.* **1996**, *8*, 327.
(37) Zhang, Y.; Haushalter, R. C.; Clearfield, A. *J. Chem. Soc., Chem. Commun.* **1996**, 1055.
(38) Zavalij, P. Y.; Chirayil, T.; Whittingham, M. S. *Acta Cryst* **1997**, *C53*, 879.

(39) Zhang, Y.; DeBord, J. R. D.; O'Connor, C. J.; Haushalter, R. C.; Clearfield, A.; Zubieta, *J. Angew. Chem., Int. Ed. Engl.* **1996**, *35*, 989.
(40) Zavalij, P. Y.; Zhang, F.; Whittingham, M. S. *Acta Crystallogr.* **1998**, in press.
(41) Chirayil, T.; Zavalij, P.; Whittingham, M. S. *Solid State Ionics* **1996**, *84*, 163.
(42) Chirayil, T.; Zavalij, P.; Whittingham, M. S. *J. Electrochem. Soc.* **1996**, *143*, L193.
(43) Bergström, Ö.; Gustafsson, T.; Thomas, J. O. *Solid State Ionics* **1998**, *110*, 179.
(44) Bouloux, J.; Milosevic, I.; Galy, J. *J. Solid State Chem.* **1976**, *16*, 393.
(45) Hagrman, D.; Zubieta, J.; Warren, C. J.; Meyer, L. M.; Treacy, M. M. J.; Haushalter, R. C. *J. Solid State Chem.* **1998**, *138*, 178.
(46) Delmas, C.; Cognac-Auradou, H.; Cocciantelli, J. M.; Ménétrier, M.; Doumerc, J. P. *Solid State Ionics* **1994**, *69*, 257.
(47) Theobald, F.; Cabala, R.; Bernard, J. *J. Solid State Chem.* **1976**, *17*, 431.
(48) Oka, Y.; Yao, T.; Yamamoto, N. *J. Solid State Chem.* **1990**, *86*, 116.
(49) Oka, Y.; Ohtani, T.; Yamamoto, N.; Takada, T. *Nippon Seramikkusu Kyokai Gakujutsu Rombunshi* **1989**, *97*, 1134.
(50) Murphy, D. W.; Christian, P. A.; Disalvo, F. J.; Carides, J. N. *J. Electrochem. Soc.* **1979**, *126*, 497.
(51) DiSalvo, F. J.; Murphy, D. W.; Waszczak, J. V. *Synth. Met.* **1979**, *1*, 29.
(52) Steele, B. C. H. *J. Phys. Colloq. (Orsay Fr.)* **1978**, *C2*, 198.
(53) Murphy, D. W.; DiSalvo, F. J.; Carides, J. N.; Waszczak, J. V. *Mater. Res. Bull.* **1978**, *13*, 1395.
(54) Zavalij, P.; Whittingham, M. S.; Boylan, E. A.; Pecharsky, V. K.; Jacobson, R. A. *Z. Kryst.* **1996**, *211*, 464.
(55) Yao, T.; Oka, Y.; Yamamoto, N. *Mater. Res. Bull.* **1992**, *27*, 669.
(56) Koene, B. E.; Taylor, N. J.; Nazar, L. F. *Angew. Chem., Int. Ed.* **1998**, in press.
(57) Riou, D.; Férey, G. *Inorg. Chem.* **1995**, *34*, 6520.
(58) Zhang, Y.; Haushalter, R. C.; Clearfield, A. *Inorg. Chem.* **1996**, *35*, 4950.
(59) Mumme, W. G.; Watts, J. A. *J. Solid State Chem.* **1971**, *3*, 319.
(60) Riou, D.; Férey, G. *J. Solid State Chem.* **1995**, *120*, 137.
(61) Zhang, Y.; O'Connor, C. J.; Clearfield, A.; Haushalter, R. C. *Chem. Mater.* **1996**, *8*, 595.
(62) Oka, Y.; Tamada, O.; Yao, T.; Yamamoto, N. *J. Solid State Chem.* **1996**, *126*, 65.
(63) Zhang, F.; Zavalij, P. Y.; Whittingham, M. S. *Mater. Res. Soc. Proc.* **1998**, *496*, 367.
(64) Zhang, F.; Zavalij, P. Y.; Whittingham, M. S. *Mater. Res. Bull.* **1997**, *32*, 701.
(65) Galy, J. *J. Solid State Chem.* **1992**, *100*, 229.
(66) Zavalij, P. Y.; Zhang, F.; Whittingham, M. S. *Acta Crystallogr.* **1997**, *C53*, 1738.
(67) Theobald, F.; Cabala, R. C. *R. Acad. Sci. Paris* **1970**, *270C*, 2138.
(68) Oka, Y.; Yao, T.; Yamamoto, N. *J. Solid State Chem.* **1990**, *89*, 372.
(69) Weeks, C. MS Thesis, State University of New York at Binghamton, 1997.
(70) Weeks, C.; Zavalij, P. Y.; Whittingham, M. S. *Inorg. Chem.* **1998**, *126*, submitted.
(71) Chirayil, T.; et al. Whittingham, M. S. unpublished work, 1997.
(72) Oka, Y.; Yao, T.; Yamamoto, N. *Mater. Res. Bull.* **1997**, *32*, 1201.
(73) Evans, H. T.; Black, S. *Inorg. Chem.* **1966**, *10*, 1808.
(74) Range, K.-J.; Eglmeier, C.; Heyns, A. M.; Waal, D. d. *Z. Naturforschung* **1990**, *45b*, 31.
(75) Oka, Y.; Yao, T.; Yamamoto, N. Proc. 1st Int. Conf. Solvothermal Reactions, Takmatsu, Japan, 13 1994.
(76) Oka, Y.; Yao, T.; Yamamoto, N. *J. Solid State Chem.* **1995**, *117*, 407.
(77) Oka, Y.; Tamada, O.; Yao, T.; Yamamoto, N. *J. Solid State Chem.* **1995**, *114*, 359.
(78) Oka, Y.; Yao, T.; Yamamoto, N.; Tamada, O. *Mater. Res. Bull.* **1997**, *32*, 59.
(79) Bouloux, J. C.; Galy, J.; Hagenmuller, P. *Rev. Chim. Miner.* **1974**, *11*, 45.
(80) Wang, X.; Liu, L.; Bontchev, R.; Jacobson, A. J. *J. Chem. Soc., Chem. Commun.* **1998**, 1009.
(81) Yoshimura, M.; Urushihara, W.; Yashima, M.; Kakihana, M. *Intermetallics* **1995**, *3*, 125.
(82) Oka, Y.; Yamamoto, N.; Ohtani, T.; Takada, T. *Nippon Seramikkusu Kyokai Gakujutsu Ronbunshi* **1989**, *97*, 1441.
(83) Yao, T.; Oka, Y.; Yamamoto, N. *J. Mater. Chem.* **1992**, *2*, 337.
(84) Babonneau, F.; Parboux, P.; Joisen, F. A.; Livage, J. *J. Chim. Phys. (Paris)* **1985**, *82*, 761.
(85) Khairy, M.; Tinet, D.; vanDamme, H. *J. Chem. Soc., Chem. Commun.* **1990**, 856.
(86) Theobald, F.; Cabala, R. *C. R. Acad. Sci. Paris* **1970**, *271*, 364.
(87) Theobald, F. *Bull. Soc. Chim. France* **1977**, 803.
(88) Cesbron, F.; Vachey, H. *Bull. Soc. Fr. Mineral. Crystallogr.* **1971**, *94*, 49.
(89) Oka, Y.; Yao, T.; Yamamoto, N. *J. Mater. Chem.* **1993**, *3*, 1037.
(90) Oka, Y.; Yao, T.; Yamamoto, N. *Nippon Seramikkusu Kyokai Gakujutsu Ronbunshi* **1990**, *98*, 1365.
(91) Yao, T.; Oka, Y.; Yamamoto, N. *J. Mater. Chem.* **1992**, *2*, 331.
(92) Oka, Y.; Yao, T.; Yamamoto, N. *J. Mater. Chem.* **1995**, *5*, 1423.
(93) Yao, T.; Oka, Y.; Yamamoto, N. *J. Mater. Chem.* **1996**, *6*, 1195.
(94) Oka, Y.; Yao, T.; Yamamoto, N. *J. Solid State Chem.* **1997**, *132*, 323.
(95) Pecquenard, B.; Zavalij, P. Y.; Whittingham, M. S. *J. Mater. Chem.* **1998**, *8*, 1255.
(96) Araki, T.; Finney, J. J.; Zoltai, T. *The Am. Miner.* **1968**, *53*, 1096.
(97) Perraud, J. *Rev. Chim. Miner.* **1974**, *11*, 302.
(98) Oka, Y.; Saito, F.; Yao, T.; Yamamoto, N. *J. Solid State Chem.* **1997**, *134*, 52.

CM980242M